STUDY OF THE BOUNDARY ELEMENT METHOD FOR THE DIRECT PROBLEM OF ELECTRICAL IMPEDANCE TOMOGRAPHY

Vanessa Rolnik , e-mail: vanessarolnik@ffclrp.usp.br
Olavo H. Menin, e-mail: olavohmenin@terra.com.br
Departamento de Física e Matemática, Faculdade de Filosofia, Ciências e Letras de Ribeirão preto - FFCLRP, Universidade de São Paulo - USP
Av. Bandeirantes, 3900 - Monte Alegre - Ribeirão Preto - SP - Brasil - CEP:14040-901

Grazieli L. C. Carosio, e-mail: gracarosio@yahoo.com.br
Paulo Seleghim Junior, e-mail: seleghim@sc.usp.br
Núcleo de Engenharia Térmica e Fluidos, Escola de Engenharia de São Carlos - EESC,
Universidade de São Paulo - USP
Av.Trabalhador São-carlense, 400 - Centro - São Carlos - SP - Brasil - CEP:13560-970

Abstract. *The main objective of this paper is to contribute to the development of a reconstruction method for the electrical impedance tomography (EIT) problem using the boundary element method (BEM). The idea is to adopt BEM to improve the performance of the solution of the direct problem. The EIT problem is generally formulated as an inverse problem and the approach to its solution consists in minimizing an error functional that confronts two different models of the same problem, one calculated from a numerical method and another experimentally obtained. An iterative process is performed until the global minimum (sought image) of the error functional has been reached. Therefore, the direct problem is solved many times to reconstruct the image, and the improvement of its performance is essential to obtain solutions in viable time. BEM can provide this benefit since it effectively reduces the dimension of the numerical problem and, consequently, results in a considerable reduction in the number of variables required for the solution. Tests with the developed BEM algorithm considering a two-dimensional domain with piecewise constant conductivities, synthetic data for the experimental setup and different values and distribution of the contrast have been performed. The first test compares the numerical results with analytical solutions for three examples and shows the validation and versatility of the implemented program. The second test simulates a simple problem of EIT and shows that the minimum of error functional occurs when the numerical image approximate of the real image. Therefore, the numerical results shows that the method is quite promising.*

Keywords: *electrical impedance tomography; boundary element methods; direct problem; multiphase flow*

1. INTRODUCTION

The principle of the EIT technique consists in applying an electric voltage (or current) excitation profile through electrodes positioned on the external surface of the object (for example, body or pipe), whose interior one wishes to know, and measuring the corresponding response (electric current flux or voltage) on the same surface. The data obtained from this procedure are supplied to a computer with specific software that reconstructs the original image, which is the distribution of the electric contrast inside the object.

Tomography by electrical sensing represents a technique of great potential for the optimization of the process usually associated with petroleum and chemical industries and medical applications as a monitoring technique on biological tissues. The EIT technique is appropriated specially to industrial processes, mainly due to its low cost of installation and maintenance, easy utilization, sufficient robustness and use in hostile regions. This technique allows the monitoring of the conditions of the flow inside pipes or the concentration and distribution of particles in tanks, as well as determining the phase inversion of the flow in oil-water flows, among others (Bennet and Williams, 2004; Tapp et al.,2003).

The image reconstruction of the conductivity distribution with EIT can be considered a two-part process (Dong et al., 2005). The first is the direct problem, in which it is calculated the electric potential inside the domain with the approximated conductivity distribution, imposing the values of the potential on the boundary. The second is the inverse problem, in which it is reconstructed the internal conductivity distribution.

The inverse problem of the EIT problem can be treated as a global minimization in which the fitness function is an error functional that expresses the difference between the actual measurements experimentally obtained and the approximated measurements numerically obtained from a prospective contrast distribution. The global minimum of the error functional corresponds to the sought image. The mathematical formulation of the EIT problem as an inverse problem is nonlinear and ill-posed (Borcea,2002). This characteristic demands a powerful optimization method which will be iteratively solved.

In this optimization process, the objective function will be evaluated thousands of times to reconstruct each image and each evaluation corresponds to the solution of a new direct problem. Therefore, the direct problem needs to be extremely fast.

The direct problem generally does not have an analytical solution to complex geometries and boundary conditions. The

alternatives to solve the equations of the direct problem are the numerical techniques including finite difference methods (FDM) and finite element method (FEM). Both are often time-consuming and require extensive computational resources and discretization of the whole domain, which is associated with unknown values of the electric potential. Accuracy requires a large number of variables to be used for the discretization (Duraiswami, Sarkar and Chahine, 1998). Besides, FDM are awkward for arbitrary boundary shapes (Dong et al., 2005).

Another alternative employed in this work is the boundary element method (BEM), which offers great flexibility for arbitrary geometries and boundary shapes. The BEM approach is, in a way, a natural choice since the boundaries that are discretized in this boundary investigation approach are only the unknowns of the inverse problems (Kolehmainen et al., 1999).

BEM converts the field equations to integral equations posed on the boundary of the domain, and effectively reduces the dimension of the numerical problem. Only the boundaries of the domain need to be discretized, resulting in a considerable reduction in the number of variables required for an accurate solution. Moreover, a solution on the boundary (electric current flux or voltage) is calculated first, and then the solution at domain points (if required) is found as a separate step. In opposition to the finite element method (FEM), which is the one mostly used in the EIT problem, the entire domain mesh is required and the entire domain solution is calculated as part of the solution.

BEM is the most recent numerical method to solve partial differential equations. It was developed by Brebbia and Dominguez, who published the first books about the technique (Brebbia, 1978; Brebbia and Dominguez, 1989). Since then, BEM has become popular and considered for the EIT problem, for example in (Babaeizadeh and Brooks, 2007; Clerc et al., 2005; Eckel and Kress, 2007).

In this context, the aim of this paper is to contribute to the improvement of the reconstruction algorithm. Specifically, it presents some results that confirm the efficiency of the boundary element method to the direct problem of EIT.

2. STATEMENT OF THE PROBLEM

The governing equation of an electrical impedance tomography problem can be derived from Maxwell equations, according to

$$\vec{\nabla} \cdot \left(-\sigma \vec{\nabla} \phi \right) = 0 \qquad \text{in} \quad \Omega, \tag{1}$$

where ϕ and σ are 3D scalar functions that represent, respectively, the electric potential and the medium's contrast (for example, the electric conductivity) and Ω represents the domain problem or the sensing volume.

The interaction between Ω and the exterior occurs through boundary $\partial\Omega$ and is defined by electrical excitation and response

$$\phi = \overline{\phi} \qquad \text{in} \quad \partial\Omega, \tag{2}$$

$$-\sigma \frac{\partial \phi}{\partial n} = \overline{J} \qquad \text{in} \quad \partial\Omega. \tag{3}$$

In Equations (2) and (3), $\overline{\phi}$ denotes the voltage profile, $\overline{J}$ is the normal component of the electric current flux and $\frac{\partial \phi}{\partial n}$ is the normal derivative.

The excitation-response can be mathematically modeled through the Dirichlet-to-Neumann map, in which the voltages $\overline{\phi}$ are imposed and the current fluxes $\overline{J}$ are calculated in the whole boundary. Otherwise, if the current fluxes $\overline{J}$ are imposed and the voltages $\overline{\phi}$ are calculated in the whole boundary, the model is known as Neumann-to-Dirichlet map. It is also possible to have a mixed map.

The distribution of conductivity σ, which corresponds to the sought image, can not be accessed directly through a formulation (Equations (1) - (3)), as both σ and ϕ are unknown. One way to obtain σ is by treating the problem as an inverse problem and adopting an error functional that compares measurements obtained from experimental and mathematical models.

Specially in the Dirichlet-to-Neumann map, the first model corresponds to a collection of measurements, $\mathbf{J}_{actual}$, which is the external flux resultant from the experimental assembly that contains the actual medium's contrast (σ_{actual}). The second model consists in calculating $\overline{\mathbf{J}}$, which corresponds to the values of the external flux calculated from the numerical model by applying prospective values of σ (σ_{approx}) to the formulation.

Therefore, the error functional is defined as

$$e = \|\mathbf{J}_{actual} - \overline{\mathbf{J}}\|. \tag{4}$$

By adjusting σ_{approx} to σ_{actual} within an acceptable error level, it is possible to conclude that

$$\sigma_{actual} \approx \sigma_{approx} \Rightarrow \mathbf{J}_{actual} \approx \overline{\mathbf{J}} \Rightarrow e \approx 0, \tag{5}$$

or also, that σ_{approx} indicates the global minimum of e.

There are two approaches to trate the boundary in the two-phase flow problem: considering σ constant and the boundary includes all interfaces between the fluids, as ilustrated in Fig. 1(a), and assuming σ with two different values (σ_{int} for the fluid inside the inclusions and σ_{ext} for the remainder domain) and the boundary is uniquely formed by the walls of the pipe, as ilustrated in Fig. 1(b). The adopted approach in this work makes the values of σ constant in Eq. (1) and the boundary includes the interfaces between the phases. For example, in the air-water flow, the conductivity of the air is considered null and the inclusions of air are interpreted as the exterior of the domain. In this case, Eq. (1) is simplified to a Laplace's equation and the reconstruction of the image consists in finding the position and extension of the internal boundaries

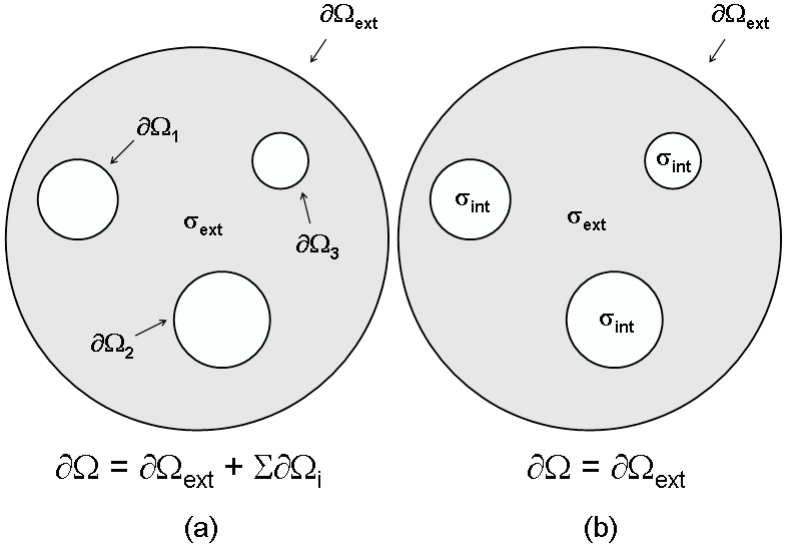

Figure 1. Two approaches: (a) constant σ and the boundary includes the interfaces between the phases and (b) non-constant σ and boundary is uniquely formed by the walls of the pipe.

3. BOUNDARY ELEMENT METHOD

Considering the two-dimensional version with constant σ in the whole domain, Eq. (1) becomes the Laplace equation

$$\frac{\partial^2 \phi}{\partial x^2} + \frac{\partial^2 \phi}{\partial y^2} = 0. \tag{6}$$

The procedure to obtain the integral equations of BEM is based on the book by Ang (2007). Firstly, a particular solution of Eq. (6), denominated fundamental solution, is obtained converting coordinates x and y to polar coordinates r and θ centered on (ξ, η), in the form

$$x = \xi + r\cos\theta \qquad \text{and} \qquad y = \eta + r\sin\theta$$

For the case in which ϕ is independent of the θ (isotropic medium), one solution of the Eq. (1) is

$$\phi(r) = \frac{1}{2\pi}\ln(r) \tag{7}$$

where $r = \sqrt{(x-\xi)^2 + (y-\eta)^2}$. Thus, the fundamental solution of the Eq. (1) can be write like Eq. (8).

$$\Phi(x, y; \xi, \eta) = \frac{1}{4\pi}\ln[(x-\xi)^2 + (y-\eta)^2] \qquad \text{for} \quad (x, y) \neq (\xi, \eta) \tag{8}$$

The divergence theorem for two-dimensional Laplace's equation provides a reciprocal relation between any two solutions ϕ_1 and ϕ_2 of Eq. (6) in region Ω bounded by curve $\partial\Omega$, that is,

$$\int_{\partial\Omega} \left(\phi_2 \frac{\partial \phi_1}{\partial n} - \phi_1 \frac{\partial \phi_2}{\partial n} \right) ds(x,y) = 0 \tag{9}$$

Taking $\phi_1 = \Phi(x,y;\xi,\eta)$ from the fundamental solution, Eq. (8), and $\phi_2 = \phi$, the required solution of the problem, a general formulation for the solution of the boundary value problem defined by Eqs. (1)-(3) is given by two equations. For a point (ξ,η) in the interior Ω of the domain, the Eq. (9) becomes

$$\phi(\xi,\eta) = \int_{\partial\Omega} \left[\phi(x,y) \frac{\partial}{\partial n} \left(\Phi(x,y;\xi,\eta) \right) - \Phi(x,y;\xi,\eta) \frac{\partial}{\partial n} \left(\phi(x,y) \right) \right] ds(x,y) \qquad \text{for} \quad (\xi,\eta) \in \Omega \tag{10}$$

However, for a point (ξ,η) in the boundary $\partial\Omega$ of the domain, the Eq. (9) becomes

$$\frac{1}{2}\phi(\xi,\eta) = \int_{\partial\Omega} \left[\phi(x,y) \frac{\partial}{\partial n} \left(\Phi(x,y;\xi,\eta) \right) - \Phi(x,y;\xi,\eta) \frac{\partial}{\partial n} \left(\phi(x,y) \right) \right] ds(x,y) \qquad \text{for} \quad (\xi,\eta) \in \partial\Omega \tag{11}$$

3.1 Specialized Numerical Solution of BEM for the EIT problem

The direct problem of EIT can be numerically solved through an algorithm computationally implemented. Firstly, the boundary $\partial\Omega$ is discretized in a prefixed number N of elements, $\partial\Omega^{(k)}, k = 1, 2, ..., N$, whose coordinates of the extremities of each element are supplied to the program. By convention, the elements are numbered following the anticlockwise direction to the external boundary and following the clockwise direction to the internal boundaries, so that the normal vector always points to the external domain Ω. The final extremity of the last element are made to coincide with the initial extremity of the first element for each connected boundary. Therefore, the domain and inclusions are approximated by polygons. Figure 2 shows an example where the external boundary is approximated using 6 elements and the inclusion using also 6 elements, $P_i, i = 1..14$, are the coordinates of the extremity of the elements and $\vec{n}$ is the normal vector.

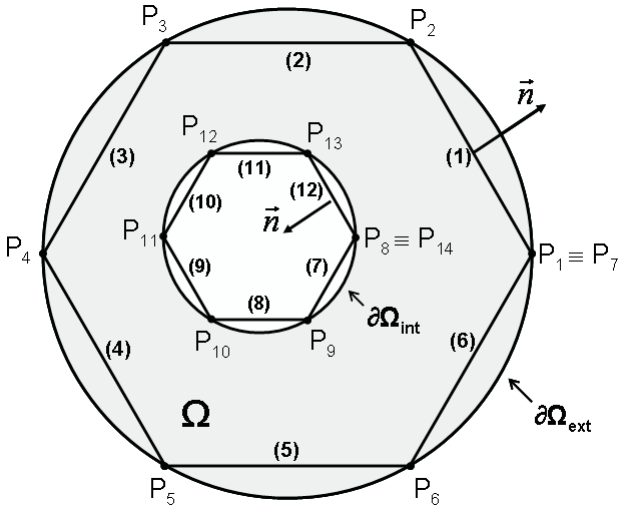

Figure 2. Example of discrete domain.

The boundary conditions are imposed considering constant values of $\overline{\phi}$ in Eq.(2) at the midpoint of element k, $(\overline{x}^{(k)}, \overline{y}^{(k)})$ or constant values of $\overline{J}$ in Eq.(3), depending on the boundary condition imposed on the element, that is,

$$\overline{\phi}^{(k)} = \phi(\overline{x}^{(k)}, \overline{y}^{(k)}) \qquad \text{for} \quad k = 1, 2, ..., N \tag{12}$$

$$\overline{J}^{(k)} = -\sigma \frac{\partial \phi}{\partial n}(\overline{x}^{(k)}, \overline{y}^{(k)}) \qquad \text{for} \quad k = 1, 2, ..., N \tag{13}$$

However, both $\overline{\phi}$ and $\overline{J}$ must be known in all elements to solve the problem in the internal points. Therefore, to obtain the unknown boundary condition on each discrete piecewise of boundary $\partial\Omega^{(k)}$, the Eq. (11) must be used considering

(ξ, η) as the midpoint of each element, $(\overline{x}^{(k)}, \overline{y}^{(k)})$. The resultant equation is

$$\frac{1}{2}\overline{\phi}^{(k)} = \sum_{k=1}^{N}\left[\overline{\phi}^{(k)}\int\limits_{\partial\Omega^{(k)}}\frac{\partial}{\partial n}[\Phi(x,y;\overline{x}^{(k)},\overline{y}^{(k)})]ds(x,y) - \overline{J}^{(k)}\int\limits_{\partial\Omega^{(k)}}\Phi(x,y;\overline{x}^{(k)},\overline{y}^{(k)})ds(x,y)\right] \tag{14}$$

for $k = 1, 2, ..., N$.

Equation (14) constitutes a system of N linear algebraic equations containing N unknowns.

The solution on the boundary is calculated first, and then the solution at the internal points (if required) is found as a separate step. After obtaining the pair $(\overline{\phi}^{(k)}, \overline{J}^{(k)})$ for all elements, the solution of the direct problem of EIT is complete, since the internal values of ϕ are not necessary. However, if the solution at some internal point (ξ, η) is required, Eq. (10) can be used in the form

$$\phi(\xi,\eta) = \sum_{k=1}^{N}\left[\overline{\phi}^{(k)}\int\limits_{\partial\Omega^{(k)}}\frac{\partial}{\partial n}[\Phi(x,y;\xi,\eta)]ds(x,y) - \overline{J}^{(k)}\int\limits_{\partial\Omega^{(k)}}\Phi(x,y;\xi,\eta)ds(x,y)\right] \tag{15}$$

for $k = 1, 2, ..., N$.

The integrals in Eq. (14) - (15) are generally solved numerically using, for instance, the quadrature of Gauss. However, this work uses an analytical solution for the integrals, given by Ang (2007).

The general steps of the program can be enumerated as:

Step 1: define the coordinates $(x^{(k)}, y^{(k)})$ of the initial extremity of each boundary element;

Step 2: calculate the average points $(\overline{x}^{(k)}, \overline{y}^{(k)})$ and normal unitary vector $[n_x, n_y]$ of each boundary element;

Step 3: define the type and the value of the boundary condition (Dirichlet ou Neumann) of each boundary element;

Step 4: calculate the integrals of Eq. (14);

Step 5: construct the linear system to determine $\overline{\phi}$ or $\overline{J}$ of each boundary element;

Step 6: solve the linear system;

Step 7: define the internal points (ξ, η);

Step 8: calculate the integrals of Eq. (15);

Step 9: calculate the approximated values of $\phi(\xi, \eta)$.

It is important to observe that the matrix of the linear system constructed in Step 5 depends on the coordinates of the boundary elements and on the type of the boundary condition imposed. An important consequence is that the dimension of the linear system does not depend on the number of internal points where the solution will be calculated, that is, the internal mesh can be considerably fine and the method may reach a solution with great accuracy using relatively few boundary elements.

Another characteristic is that the linear system is solved once, in Step 6, and does not need to be solved again during the calculation of ϕ in the points of the internal mesh, independently of the number of these points.

4. NUMERICAL RESULTS

A program has been implemented using C language, based on the routines presented by Ang (2007) and Brebbia and Dominguez (1989). To solve the linear system generated by Eq. (14), the Gaussian elimination with partial pivoting was implemented. The first numerical tests showed the validation of the program considering three examples which have analytical solutions. However the most important goal of these examples is to show how versatile the program is, as it admits boundary conditions of Dirichlet, Neumann or mixed types, rectangular and circular domains. In fact, the program admits any geometry of the external and internal boundaries since each one is a simple closed curve.

The three boundary value problems (BVPI)-(BVPIII) used in this stage are:

$$\text{(BVP I)} \begin{cases} \nabla^2\phi = 0 & (x,y) \in \Omega = [0,1]\times[0,1] \\ \phi(x,0) = 0 & \text{for} \quad x \in [0,1] \\ \phi(0,y) = 0 & \text{for} \quad y \in [0,1] \\ \phi(x,1) = x & \text{for} \quad x \in [0,1] \\ \phi(1,y) = y & \text{for} \quad y \in [0,1] \end{cases}$$

The analytical solution of BVP I is $\phi(x,y) = x.y$.

$$\text{(BVP II)} \begin{cases} \nabla^2\phi = 0 & (x,y) \in \Omega = [0,1]\times[0,1] \\ \phi(0,y) = 0 & \text{for} \quad y \in [0,1] \\ \phi(1,y) = cos(\pi\, y) & \text{for} \quad y \in [0,1] \\ \frac{\partial\phi}{\partial n}(x,0) = 0 & \text{for} \quad x \in [0,1] \\ \frac{\partial\phi}{\partial n}(x,1) = 0 & \text{for} \quad x \in [0,1] \end{cases}$$

The analytical solution of BVP II is $\phi(x,y) = \frac{senh(\pi\, x)cos(\pi\, y)}{senh(\pi)}$.

$$\text{(BVP III)} \begin{cases} \nabla^2\phi = 0 & (x,y) \in \Omega = \{(x,y) \in R^2; x^2+y^2 \leq 1\} \\ \phi(x,y) = x+y & \text{for} \quad (x,y) \in \partial\Omega = \{(x,y) \in R^2; x^2+y^2 = 1\} \end{cases}$$

The analytical solution of BVP III is $\phi(x,y) = x + y$.

For BVP I and BVP II, the program calculates the approximate solution in 400 internal points uniformly distributed in a 20×20 Cartesian mesh. For BVP III, the program generated a square mesh of 23×23 points centered in the origin of the Cartesian system (the origin coincides with the center of the circular domain) and the solutions are calculated only in the mesh points located in the interior of the domain. Therefore, the number of evaluated internal points in BVP III is variable depending on the number of boundary elements.

A relative error, Eq. (16), was used to compare the analytical and numerical solutions in all evaluated points and shows the accuracy of the results.

$$RE = \frac{|\phi_{actual} - \phi_{approx}|}{|max\{\phi_{actual}\} - min\{\phi_{actual}\}|} \tag{16}$$

The program was run for the three BVP and for different values of the number of boundary elements (**N**). The maximum relative error of each test is presented in Tab. 1. The error values are also plotted and can be seen in Fig. 3, where the relative error axes are on a logarithmic scale.

Table 1. Decrease in the maximum relative error for the three BVP varying the number of elements.

N	**8**	**16**	**24**	**32**	**40**	**48**	**56**
BVP I	0.12627202	0.03479151	0.01161412	0.00345948	0.00089747	0.00041890	0.00031500
BVP II	0.13079459	0.02887951	0.00868101	0.00504889	0.00264197	0.00206198	0.00139268
BVP III	0.04164375	0.02057055	0.01342036	0.00469346	0.00597683	0.00256674	0.00355676
N	**64**	**72**	**80**	**120**	**160**	**200**	**240**
BVP I	0.00020005	0.00009505	0.00003758	0.00000995	0.00000442	0.00000221	0.00000111
BVP II	0.00119112	0.00107359	0.00090436	0.00049537	0.00032143	0.00022859	0.00017217
BVP III	0.00154004	0.00201672	0.00095336	0.00058668	0.00007334	0.00011000	0.00003667

Figure 3 shows that the relative error decreases significantly when the number of boundary elements increases. The program was also tested for more than 240 boundary elements. However, for $\mathbf{N} > 240$ the results do not present significant variations in relative error. Each test took less than one second of computational time to carried out.

The second test simulates a two-phase flow inside a unitary square pipe. For the purpose of test, the domain was placed in the $[0.0, 1.0] \times [0.0, 1.0]$ set in a Cartesian coordinates system with one inclusion inside the domain (gray area in Fig. 4 simulating one "square" bubble with side of 0.11) defined for the region $[0.61, 0.72] \times [0.61, 0.72]$.

The external boundary was discretized in 80 elements (20 per side) and the internal boundary in 16 elements (4 per side), generating $\mathbf{N} = 96$ elements. The electric voltage excitation profile adopted is the diametrical (also called

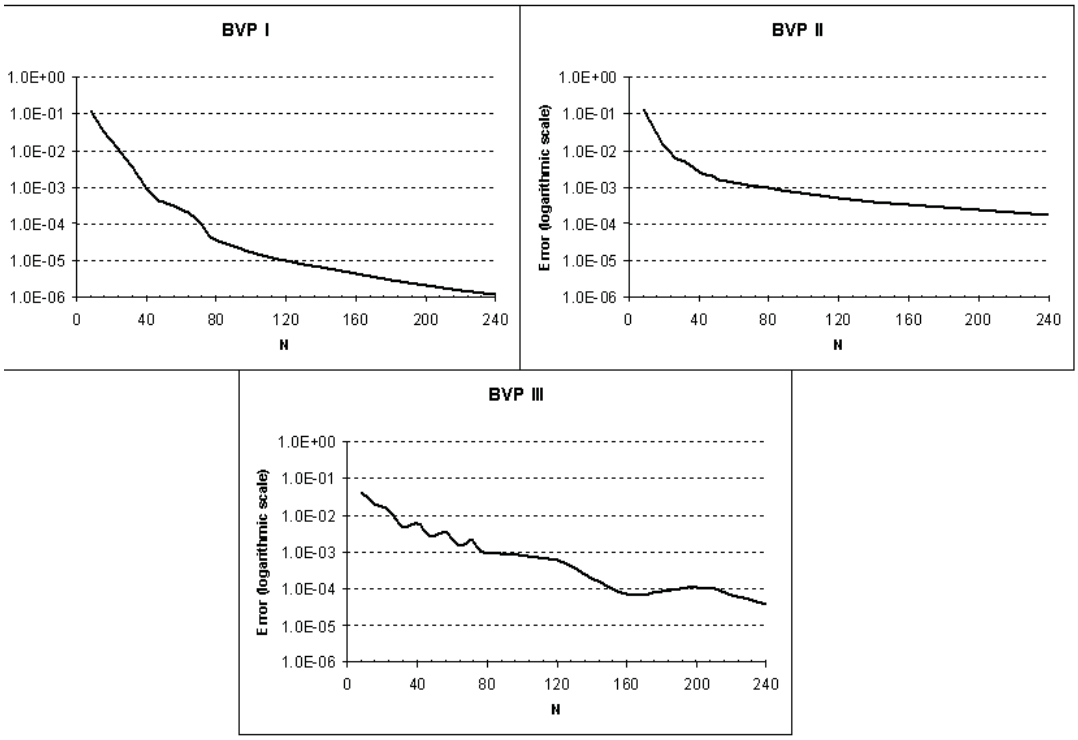

Figure 3. Relation between the maximum relative error and the number of elements for BVP I, BVP II and BVP III.

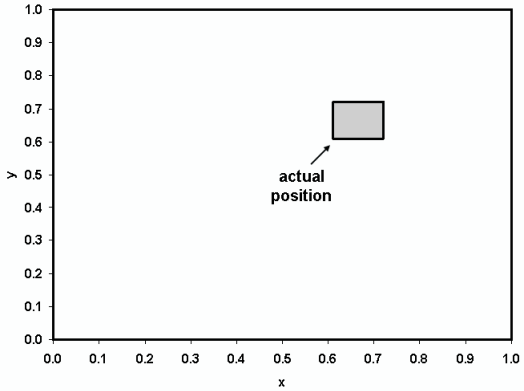

Figure 4. Actual position of the inclusion inside the domain.

triangular) configuration. This profile was numerically simulated as a voltage of $10V$ emitted from the electrode located in the superior right corner of the square and gradually decreasing to a minimum value ($0V$) in the electrode diametrically opposed to it. The advantage of this configuration is that it allows the electric field to pass through the sensing domain to be more sensitive to changes inside the domain, detecting the electrical contrast distribution better (Figueroa and Seleghim Junior, 2001). Figure 5 shows the potential imposed on the external boundary related to the elements. It is important to observe that the null fluxes are imposed on all elements in the internal boundary.

To evaluate the sensitivity of the BEM in relation to the approximated current flux in the external boundary, this test was based on tests of Figueroa and Seleghim (2001) and considered one prospective inclusion had been dislocated through the diagonal from the lower left corner to the upper right corner and had taken eight positions, as seen in Fig. 6. The prospective inclusion is a square with sides of 0.1 and the coordinates of lower left corners of each position were, respectively, $(0.1, 0.1)$, $(0.2, 0.2)$, $(0.3, 0.3)$, $(0.4, 0.4)$, $(0.5, 0.5)$, $(0.6, 0.6)$, $(0.7, 0.7)$ and $(0.8, 0.8)$. This figure also shows the best approximation to the actual position of the inclusion.

The error functional, Eq. (4), compares the $\mathbf{J}_{\mathbf{actual}}$ obtained with the inclusion in the actual position and $\overline{\mathbf{J}}$ calculated for each position of the prospective inclusion. Figure 7 presents a graph of the normalized values obtained for functional e at the eight positions of the prospective inclusion.

Figure 7 corroborates the observation that position 6 is the best approximation for the actual position. Furthermore, when the prospective position approaches the actual position, the value of the error functional decreases. Finally, in this

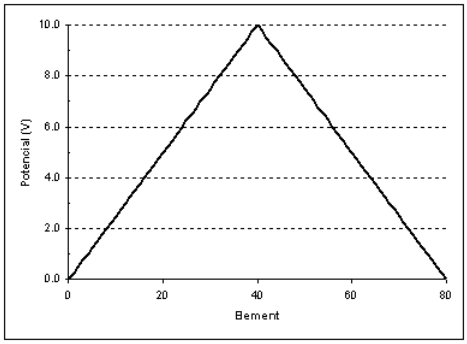

Figure 5. Triangular electric voltage excitation profile on the 80 elements of the external boundary.

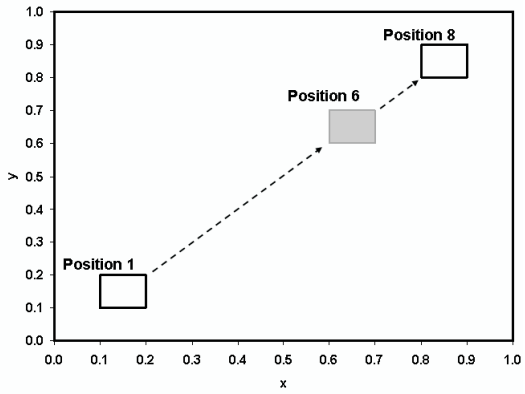

Figure 6. Prospective inclusion set in 8 positions in the diagonal of the square and the best approximation.

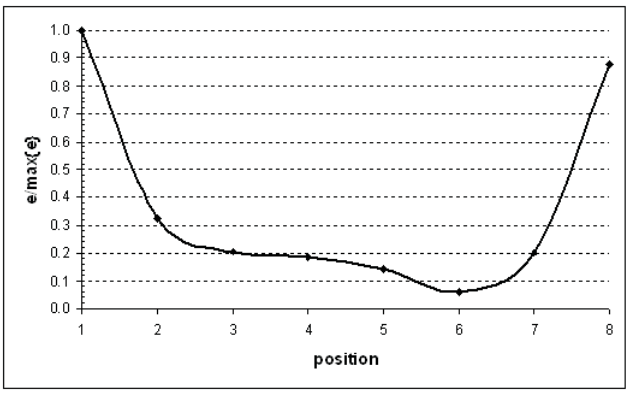

Figure 7. Normalized values of functional e for the eight positions of the prospective inclusion.

test the prospective inclusion never occupies exactly the actual position, thus the lowest value of the error functional is not zero.

5. CONCLUSIONS

For the validation of the program developed, considering three BVP, tests have shown that BEM is a versatile program since it admits boundary conditions of Dirichlet, Neumann or mixed types and rectangular and circular domains. In fact, the program admits any geometry of the external and internal boundaries since each one is a simple closed curve.

Also, BEM produces results that are sensitive in relation to the approximated current flux in the external boundary. Specifically, one prospective inclusion was dislocated through the diagonal from the lower left corner to the upper right corner of the domain and took eight positions. Hereby, one could calculate the error functional, which compared the current flux obtained with the inclusion in the actual position and the current flux calculated for each position of the prospective inclusion. It was possible to observe that when the prospective position approaches the actual position, the value of the error functional decreases. Nowadays, the work is exploring mediums with unknown shape and quantity of

inclusions inside it. Therefore, BEM is a very promising technique to obtain the direct solution of the EIT problem.

Future works should introduce regularization techniques and an optimization method to reconstruct the image of EIT, which could be based on heuristic or deterministic methods.

6. ACKNOWLEDGEMENTS

The authors would like to acknowledge *FAPESP*, Grant No. 08/01284-4, for the financial support given to this research.

7. REFERENCES

Ang W.T., 2007, "A beginner's course in boundary element methods", Boca Raton: Universal Publishers.

Babaeizadeh, S. and Brooks, D. H., 2007, "Electrical impedance tomography for piecewise constant domains using boundary element shape-based inverse solution", IEEE Transactions on Medical Imaging, Vol. 26, No. 5, pp. 637-647.

Bennett, M. and Williams, R., 2004, "Monitoring the operation of an oil/water separator using impedance tomography", *Minerals Engineering*, Vol. 17, pp. 605-614.

Borcea, L., 2002, "Electrical impedance tomography", Inverse Problems, Vol. 18, pp. R99-R136.

Brebbia C.A., 1978, "The boundary element method for engineers", Plymonth: Pentech Press.

Brebbia C.A. and Dominguez J., 1989, "Boundary elements: an introductory course",Southampton: WIT Press.

Dong, G. et al, 2005, "The comparison between FVM and FEM for EIT forward problem", IEEE Transactions of Magnetics, Vol. 41, No. 5, pp. 1468-1471.

Clerc, M. et al, 2005, "Boundary element formulation for electrical impedance tomography", ESAIM: Proceedings, Vol. 14, pp. 63-71.

Duraiswami, R., Sarkar, K. and Chahine, L, 1998, "Efficient 2D and 3D electrical impedance tomography using dual reciprocity boundary element techniques", Engineering Analysis with Boundary Elements, Vol. 22, pp. 13-31.

Eckel, H. and Kress, R., 2007, "Nonlinear integral equations for the inverse electrical impedance tomography", Inverse Problems, Vol. 23, pp. 475-491.

Figueroa, T. and Seleghim Junior, P., 2001, Sensitivity analysis of different sensing strategies for electrical impedance imaging of two-phases flows, Journal of Electronic Imaging, Vol. 10, No. 3, pp. 641-645.

Kolehmainen, V. et al, 1999, "Recovery of region boundaries of piecewise constant coefficients of an elliptic PDE from boundary data", Inverse Problems, Vol. 15, pp. 1375-1391.

Tapp, H. et al., 2003, "Chemical engineering applications of electrical process tomography", Sensors and Actuators B: Chemical, Vol. 92, pp. 17-24.

8. Responsibility notice

The author(s) is (are) the only responsible for the printed material included in this paper